JVI Journals.ASM.org

Toll-Like Receptor 9-Mediated Protection of Enterovirus 71 Infection in Mice Is Due to the Release of Danger-Associated Molecular Patterns

Hung-Bo Hsiao,[a] Ai-Hsiang Chou,[a] Su-I Lin,[a] I-Hua Chen,[a] Shu-Pei Lien,[a] Chia-Chyi Liu,[a] Pele Chong,[a,b] Shih-Jen Liu[a,b]

National Institute of Infectious Diseases and Vaccinology, National Health Research Institutes, Zhunan, Miaoli, Taiwan[a]; Graduate Institute of Immunology, China Medical University, Taichung, Taiwan[b]

ABSTRACT

Enterovirus 71 (EV71), a positive-stranded RNA virus, is the major cause of hand, foot, and mouth disease (HFMD) with severe neurological symptoms. Antiviral type I interferon (alpha/beta interferon [IFN-α/β]) responses initiated from innate receptor signaling are inhibited by EV71-encoded proteases. It is less well understood whether EV71-induced apoptosis provides a signal to activate type I interferon responses as a host defensive mechanism. In this report, we found that EV71 alone cannot activate Toll-like receptor 9 (TLR9) signaling, but supernatant from EV71-infected cells is capable of activating TLR9. We hypothesized that TLR9-activating signaling from plasmacytoid dendritic cells (pDCs) may contribute to host defense mechanisms. To test our hypothesis, Flt3 ligand-cultured DCs (Flt3L-DCs) from both wild-type (WT) and TLR9 knockout (TLR9KO) mice were infected with EV71. More viral particles were produced in TLR9KO mice than by WT mice. In contrast, alpha interferon (IFN-α), monocyte chemotactic protein 1 (MCP-1), tumor necrosis factor-alpha (TNF-α), IFN-γ, interleukin 6 (IL-6), and IL-10 levels were increased in Flt3L-DCs from WT mice infected with EV71 compared with TLR9KO mice. Seven-day-old TLR9KO mice infected with a non-mouse-adapted EV71 strain developed neurological lesion-related symptoms, including hind-limb paralysis, slowness, ataxia, and lethargy, but WT mice did not present with these symptoms. Lung, brain, small intestine, forelimb, and hind-limb tissues collected from TLR9KO mice exhibited significantly higher viral loads than equivalent tissues collected from WT mice. Histopathologic damage was observed in brain, small intestine, forelimb, and hind-limb tissues collected from TLR9KO mice infected with EV71. Our findings demonstrate that TLR9 is an important host defense molecule during EV71 infection.

IMPORTANCE

The host innate immune system is equipped with pattern recognition receptors (PRRs), which are useful for defending the host against invading pathogens. During enterovirus 71 (EV71) infection, the innate immune system is activated by pathogen-associated molecular patterns (PAMPs), which include viral RNA or DNA, and these PAMPs are recognized by PRRs. Toll-like receptor 3 (TLR3) and TLR7/8 recognize viral nucleic acids, and TLR9 senses unmethylated CpG DNA or pathogen-derived DNA. These PRRs stimulate the production of type I interferons (IFNs) to counteract viral infection, and they are the major source of antiviral alpha interferon (IFN-α) production in pDCs, which can produce 200- to 1,000-fold more IFN-α than any other immune cell type. In addition to PAMPs, danger-associated molecular patterns (DAMPs) are known to be potent activators of innate immune signaling, including TLR9. We found that EV71 induces cellular apoptosis, resulting in tissue damage; the endogenous DNA from dead cells may activate the innate immune system through TLR9. Therefore, our study provides new insights into EV71-induced apoptosis, which stimulates TLR9 in EV71-associated infections.

Enterovirus 71 (EV71) is a small, nonenveloped virus with a single-stranded RNA genome of approximately 7.4 kb and belongs to the genus *Enterovirus* within the family *Picornaviridae*. Furthermore, EV71 causes outbreaks of hand, foot, and mouth disease (HFMD) in young children throughout the world, and this infection has exhibited significantly increased mortality in recent years, particularly in the Asia-Pacific region (1–4). As a typical neurotropic virus, EV71 has a propensity to cause neurological disease during acute infection and may lead to permanent paralysis and even death (5, 6). In recent years, large HFMD outbreaks in the Asia-Pacific region have been reported (4, 7). Additionally, neonates and infants are more susceptible than adults to infectious diseases following exposure to viruses. Severe neurological manifestations in children may arise from EV71-induced apoptosis or cytokine release (8–10). In the absence of type I interferon (alpha/beta interferon [IFN-α/β]) and type II interferon (IFN-γ) receptors, young mice develop neurological manifestations following EV71 infection. The innate receptors may play important roles in EV71 pathogenesis.

Four families of pattern recognition receptors (PRRs) are currently known: Toll-like receptors (TLRs), retinoic acid-inducible

Received 28 March 2014 Accepted 21 July 2014
Published ahead of print 30 July 2014
Editor: M. S. Diamond
Address correspondence to Shih-Jen Liu, levent@nhri.org.tw.
H.-B.H. and A.-H.C. contributed equally to this work.

doi:10.1128/JVI.00867-14
The authors have paid a fee to allow immediate free access to this article.

gene I (RIG-I)-like receptors (RLRs), nucleotide-binding oligomerization domain (NOD)-like receptors (NLRs), and HIN-200 family members (11). During viral infection, innate immunity is activated by the recognition of pathogen-associated molecular patterns (PAMPs), which include viral RNA and DNA, by PRRs. Endosomal TLRs (TLR3, TLR7, TLR8, and TLR9) and cytoplasmic RNA sensor RLRs (RIG-I and MDA5) recognize viral nucleic acids. TLR3, RIG-I, and MDA5 recognize double-stranded RNA (dsRNA) and stimulate the production of type I IFNs (12–14). TLR7/8 recognize single-stranded RNA (ssRNA) and induce production of type I IFNs and cytokines in plasmacytoid DCs (pDCs) (15). TLR9, absent in melanoma 2 (AIM2), and stimulator of IFN gene (STING) recognize pathogen-derived DNA to activate the production of type I IFN (16). In addition to PAMPs, danger-associated molecular patterns (DAMPs) are known to be potent activators of innate immune signaling (17). DAMPs arise from cellular injury or necrosis and include high-mobility group box protein 1 (HMGB1), heat shock proteins (HSPs), and DNA (18). These findings indicate that the innate immune response could be induced directly by viral components or indirectly by cellular components following viral infection.

Induction of IFNs is an important mechanism for the control of viral infections. Although IFN receptor knockout mice infected with non-mouse-adapted EV71 exhibit neurological manifestations and progress to death in 2-week-old mice (19), a limited number of studies have identified the innate receptors responsible for the secretion of IFNs. Signaling from TLR3 and RIG-I has been proposed to be inhibited by EV71 components, allowing the virus to escape the antiviral innate response of the host (20, 21). In addition to TLR3 and RIG-I, other innate receptors may be responsible for the secretion of IFNs following EV71 infection. The pDC population is the major source of antiviral IFN-α, and these cells can produce 200- to 1,000-fold more IFN-α than any other blood cell type (22, 23). The high expression levels of TLR7 and TLR9 in pDCs allow the cells to detect various forms of viral nucleic acids in endosomal compartments (24, 25). However, TLR3 expression can be detected in conventional DCs, but not in pDCs (26). EV71 also induces cellular apoptosis, which results in tissue damage (8, 27, 28). This tissue damage leads to the release of endogenous DNA from dead cells, which can then activate the innate immune system through TLR9 (29). Thus, we investigated whether EV71-induced apoptosis could stimulate TLR9 in EV71-associated immunopathogenesis.

In the present study, we demonstrate that pDCs incubated with supernatant derived from EV71-infected cells activate the nuclear factor κB (NF-κB) signaling pathway. EV71 replication was increased in EV71-infected pDCs from TLR9 knockout (TLR9KO) mice compared with pDCs from wild-type (WT) mice. The infection of 7-day-old TLR9KO mice with EV71 induced a neurological disease progression that was similar to the human disease progression. Therefore, we hypothesized that TLR9 mediates the production of IFN-α in pDCs following EV71 infection and the release of endogenous DNA from necrotic and/or apoptotic cells.

MATERIALS AND METHODS

Virus and cells. EV71 strains 4643 (Tainan/4643/98 genotype C2) and 5746 (Tainan/5746/98 C2) were used in this study. EV71 4643 was derived from a nonfatal case with central nervous system (CNS) involvement (30). EV71 5746 was derived from a child with HFMD (30). Viral growth experiments were performed in African green monkey kidney (Vero) cells (ATCC CCL-81), and virus purification was conducted as previously described (31). Vero cells were cultured in VP-SFM medium (Gibco-Invitrogen, CA, USA) supplemented with 4 mM L-glutamine (Gibco-Invitrogen, CA, USA). The virus stocks were stored at −80°C. Viral titers were determined by plaque assay using rhabdomyosarcoma (RD) cells (19), and titers were expressed as PFU per milliliter.

Preparation of sEV71-RD. RD cells were cultured in Dulbecco's modified Eagle's medium containing 10% fetal bovine serum (FBS). The RD cells were plated in 6-well plates and infected with EV71 4643 at an MOI of 50 and then cultured for 48 h. After 48 h, the supernatant was collected and centrifuged at 1,500 × *g* for 10 min to remove cellular debris. EV71 in the supernatants from EV71-infected RD cells (sEV71-RD) was inactivated by UV light for 30 min or heated at 56°C for 30 min (32, 33). The sEV71-RD was stored at −80°C.

NF-κB dual-luciferase reporter assay. HEK293 cells or TLR9-expressing 293 cells (mTLR9/293) were plated in 24-well plates (2×10^5 cells/well) and cotransfected with 0.25 μg of pNF-kB-luc and 0.25 μg of the pRL-TK internal control plasmid (Promega, Madison, WI, USA) using the PolyJet reagent (SignaGen, MD, USA) (34). After 24 h, the transfected cells were stimulated with CpG ODN, EV71, or EV71-infected cell supernatants for 24 h. The cells were then lysed so that the luciferase activity could be measured using a dual-luciferase reporter assay system (Promega Co., Madison, WI, USA). Firefly luciferase activity was normalized to *Renilla* luciferase activity for each sample. Both firefly and *Renilla* luciferase activities were quantified using a Berthold (Pforzheim, Germany) Orion II luminometer.

Preparation and infection of Flt3L-DCs. Bone marrow was flushed from the tibias and femurs of WT or TLR9KO mice using a 24-gauge needle and RPMI 1640 medium supplemented with 10% heat-inactivated fetal bovine serum, 100 U/ml penicillin-streptomycin, and 1% L-glutamine. After red blood cell (RBC) lysis, bone marrow cells were cultured for 7 days at a concentration of 10^6 cells/ml in RPMI 1640 culture medium supplemented with 100 ng/ml recombinant murine Flt3 ligand (Flt3L) (Peprotech, USA). Cultures were maintained at 37°C in a 5% CO_2 humidified atmosphere. The purity of the pDC ($CD11c^+$ $B220^+$) population was assessed by flow cytometry and maintained at 40 to 50%. Subsequently, the bone marrow cells stimulated with Flt3 ligand (Flt3L-DCs) (5×10^5/well) were seeded in 48-well plates with a final volume of 500 μl and then exposed to EV71, mock treatment, or CpG ODN (10 μg/ml) at MOIs of 5 and 10.

Cytokine assays. After 48 h of infection, culture supernatants were harvested and assayed for secreted-cytokine levels by enzyme-linked immunosorbent assay (ELISA) according to the manufacturers' protocols. The following cytokine concentrations were determined: IFN-α (eBioscience, San Diego CA, USA), IFN-γ, monocyte chemotactic protein 1 (MCP-1), tumor necrosis factor-alpha (TNF-α), interleukin 6 (IL-6), and IL-10 (BD Cytometric Bead Array [CBA]; BD Biosciences, San Diego, CA).

Detecting the viability of Flt3L-DCs from WT and TLR9KO mice after EV71 infection. Viral infection has been shown to affect the viability of Flt3L-DCs from WT and TLR9KO mice. Bone marrow was flushed from the tibias and femurs of WT or TLR9KO mice using a 24-gauge needle and RPMI 1640 medium supplemented with 10% heat-inactivated fetal bovine serum, 100 U/ml penicillin-streptomycin, and 1% L-glutamine. After RBC lysis, bone marrow cells were cultured for 7 days at a concentration of 10^6 cells/ml in RPMI 1640 culture medium supplemented with 100 ng/ml recombinant murine Flt3 ligand (Peprotech, USA). The Flt3L-DCs (5×10^5/well) were seeded in 48-well plates in a total volume of 500 μl and infected with EV71 at an MOI of 5, 10, 20, or 50 for 24 or 48 h. We investigated the effect of EV71 infection on the viability of Flt3L-DCs using trypan blue exclusion counting at 24 or 48 h postinfection.

Mouse infection. WT and TLR9KO 7-day-old mice were obtained from the Animal Center of the National Health Research Institutes (NHRI) in Taiwan. The mice were housed under pathogen-free condi-

TABLE 1 UPL numbers and primer sequences for mRNA analysis by real-time PCR

Gene product	UPL no.	Primers[a]	
		Orientation	Sequence
IL-1β	78	Forward	5′-TGTAATGAAAGACGGCACACC-3′
		Reverse	5′-TCTTCTTTGGGTATTGCTTGG-3′
GAPDH	9	Forward	5′-GAGCCAACGGGTCATCATCT-3′
		Reverse	5′-GAGGGGCCATCCACAGTCTT-3′
IFN-α	51	Forward	5′-GCCTTAACCCTCCTGGTAAAA-3′
		Reverse	5′-TCCTGTGGGAATCCAAAGTC-3′
TNF-α	25	Forward	5′-CTGTAGCCCACGTCGTAGC-3′
		Reverse	5′-TTGAGATCCATGCCGTTG-3′
IFN-γ	21	Forward	5′-ATCTGGAGGAACTGGCAAAA-3′
		Reverse	5′-TTCAAGACTTCAAAGAGTCTGAGG-3′
IL-6	6	Forward	5′-GCTACCAAACTGGATATAATCAGGA-3′
		Reverse	5′-CCAGGTAGCTATGGTACTCCAGAA-3′
IP-10	3	Forward	5′-GCTGCCGTCATTTTCTGC-3′
		Reverse	5′-TCTCACTGGCCCGTCATC-3′
MCP-1	62	Forward	5′-CATCCACGTGTTGGCTCA-3′
		Reverse	5′-GATCATCTTGCTGGTGAATGAGT-3′
MIP-1α	40	Forward	5′-CAAGTCTTCTCAGCGCCATA-3′
		Reverse	5′-GGAATCTTCCGGCTGTAGG-3′

[a] Sequences designed for the detection of the indicated gene products by real-time PCR are presented.

TABLE 2 Primer sequences of TLRs for mRNA analysis by real-time PCR

Gene product	Primers	
	Orientation	Sequence
TLR1	Forward	5′-TCTTCGGCACGTTAGCACTG-3′
	Reverse	5′-CCAAACCGATCGTAGTGCTGA-3′
TLR2	Forward	5′-GGGGCTTCACTTCTCTGCTT-3′
	Reverse	5′-AGCATCCTCTGAGATTTGACG-3′
TLR3	Forward	5′-GATACAGGGATTGCACCCATA-3′
	Reverse	5′-TCCCCCAAAGGAGTACATTAGA-3′
TLR4	Forward	5′-GGACTCTGATCATGGTAGGT-3′
	Reverse	5′-CTGATCCATGCATTGGTAGGT-3′
TLR5	Forward	5′-TCATGGATGGATGCTGAGTT-3′
	Reverse	5′-TGGCCATGAAGATCACACC-3′
TLR6	Forward	5′-GGTACCGTCAGTGCTGGAA-3′
	Reverse	5′-GGGTTTTCTGTCTTGGCTCA-3′
TLR7	Forward	5′-GATCCTGGCCTATCTCTGACTC-3′
	Reverse	5′-CGTGTCCACATCGAAAACAC-3′
TLR8	Forward	5′-CAAACGTTTTACCTTCCTTTGTC-3′
	Reverse	5′-ATGGAAGATGGCACTGGTTC-3′
TLR9	Forward	5′-GAATCCTCCATCTCCCAACAT-3′
	Reverse	5′-CCAGAGTCTCAGCCAGCACT-3′

tions in individual ventilated cages. Animal use protocol was reviewed and approved by the NHRI Institutional Animal Care and Use Committee (NHRI-IACUC-099110-A), and institutional guidelines for animal care and use were strictly followed. Six groups ($n = 6$ or 7 per group) were inoculated via intraperitoneal (i.p.) injection with 1×10^7 PFU of EV71 4643 or EV71 5746. The animals were observed twice daily for 21 days for clinical symptoms, weight changes, and mortality. Clinical scores were defined as follows: 0, healthy; 1, ruffled hair, hunchbacked, or reduced mobility; 2, limb weakness; 3, paralysis in 1 limb; 4, paralysis in both limbs; and 5, death. Each group contained 6 or 7 WT and TLR9KO 7-day-old mice.

Histology. Organs and tissues were harvested from euthanized mice and immediately incubated in 4% formalin for 48 h. The fixed tissues were embedded in paraffin, sectioned, and stained with hematoxylin and eosin (H&E).

Determination of viral titers in infected mice. Euthanized animals were perfused systemically with 50 ml of sterile phosphate-buffered saline (PBS) prior to organ harvesting at 3, 7, and 11 days postinfection (p.i.). The tissue samples were homogenized in sterile phosphate-buffered saline (PBS) (10% [wt/vol]), disrupted by three freeze-thaw cycles, and centrifuged. Viral titers in the supernatants of clarified homogenates were determined by plaque assay, as described above, and expressed as PFU per gram or per ml. The limit of sensitivity was determined to be 20 PFU.

Real-time qPCR. At 3, 7, and 11 days p.i., brain samples from each group of WT and TLR9KO 7-day-old mice and WT and TLR9KO Flt3L-DCs were collected and analyzed. Total RNA was isolated to detect TNF-α, IFN-γ, IFN-α, IL-6, IL-1β, MIP-1α, MCP-1, and IP-10 transcript levels. The mouse Universal Probe Library (UPL) set (35) was used to perform real-time quantitative PCR (qPCR) to detect TNF-α, IFN-γ, IFN-α, IL-6, IL-1β, MIP-1α, MCP-1, and IP-10 gene expression. The specific primers and the UPL catalog numbers are listed in Table 1. The expression of TNF-α, IFN-γ, IFN-α, IL-6, IL-1β, MIP-1α, MCP-1, and IP-10 genes was calculated using the comparative method to quantify relative expression after normalization to glyceraldehyde-3-phosphate dehydrogenase (GAPDH) gene expression. We determined the TNF-α, IFN-γ, IFN-α, IL-6, IL-1β, MIP-1α, MCP-1, and IP-10 transcript levels in the brains of WT and TLR9KO 7-day-old mice.

Isolation of pDCs. Adult and neonatal spleens were harvested from 6-week-old or 7-day-old C57BL/6 WT mice, respectively, using the anti-mouse PDCA1 (mPDCA1) microbead kit (Miltenyi Biotec GmbH, Germany) according to the protocol from Miltenyi Biotec. Briefly, splenocytes were crushed in LCM (RPMI 1640 medium supplemented with 10% FBS, 100 U/ml penicillin-streptomycin, 2 mM glutamine, 10 mM HEPES, and 50 μM 2-mercaptoethanol [2-ME]) and strained through a 70-μM filter. RBCs were removed by incubation in ammonium–chloride–potassium (ACK) lysis buffer. The isolated splenocytes were maintained throughout the procedure in cold PBS-bovine serum albumin (BSA)-EDTA. The cells were labeled with anti-mouse PDCA1 microbeads and then washed and positively selected using magnetic-separation LS columns and a MACS Separator (Miltenyi Biotec GmbH, Germany).

Detection of TLR expression by real-time qPCR. RNA was extracted from purified pDCs using TRIzol reagent. Total RNA was reverse transcribed into cDNA using Moloney murine leukemia virus (MMLV) reverse transcriptase (Genemarkbio, Taiwan) to detect TLR transcript levels. SYBR green PCR master mix was used to conduct real-time qPCR to quantify the expression levels of TLR1 to -9. The specific primers are listed in Table 2. The expression levels of TLR1 to -9 were calculated using the comparative method for relative quantification after normalization to GAPDH gene expression.

Depletion of pDCs in mice by anti-PDCA1 antibody. Purified anti-mouse CD317 (PDCA1)(BioLegend, CA, USA) was used to deplete pDCs *in vivo*. Five-day-old mice were first treated with one dose (5 mg/kg body weight) of anti-mouse CD317 via i.p. injection, and then the same dose was repeated the next day (36). Control antibody (purified rat IgG1; eBioscience, CA, USA) and untreated mice were used as control groups in the experiment. All of the mice were infected with 1×10^7 PFU of EV71 (strain 4643-TW98) at day 7 of life.

Statistical analysis. Statistical data are expressed as means and standard deviations (SD). Statistical analyses were performed using Prism 5 software (GraphPad, San Diego, CA). Body weight changes and clinical-score curves were analyzed by the Wilcoxon test. All other data were analyzed using Student's *t* test.

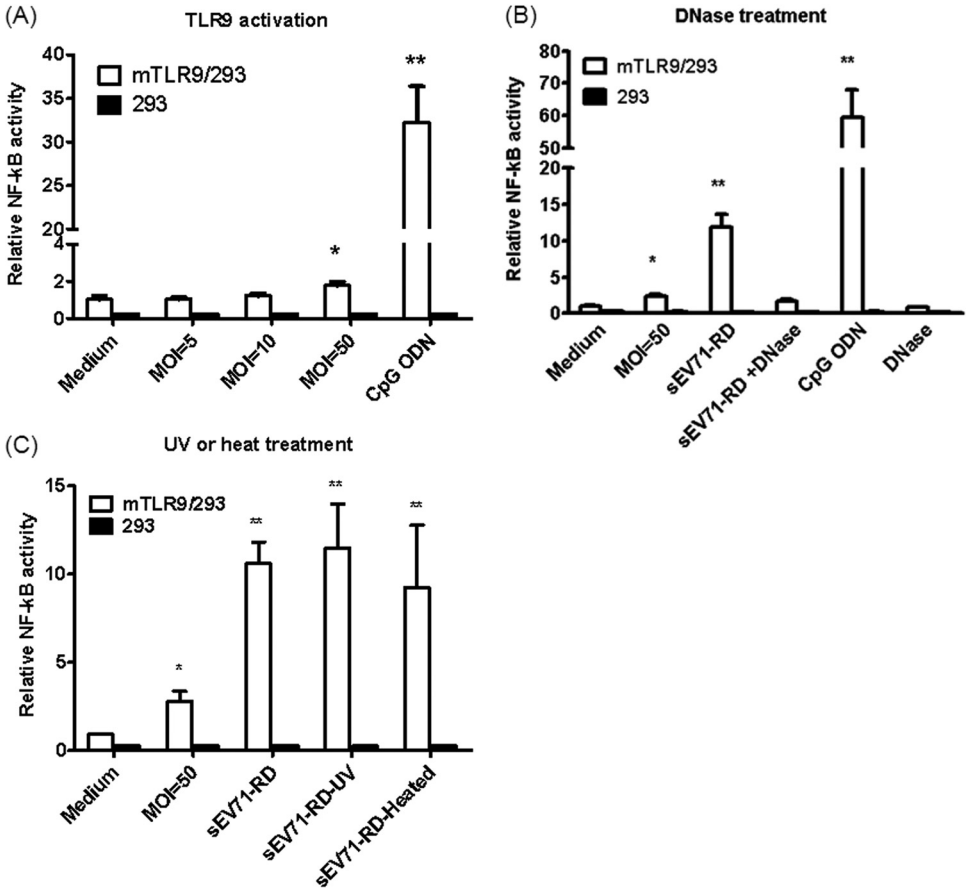

FIG 1 Supernatants from EV71-infected cells activate TLR9 signaling. mTLR9/293 cells were transfected with 0.25 μg of pNF-kB-luc and 0.25 μg of the pRL-TK internal control plasmid. After 24 h, the cells were cultured with various reagents for another 24 h, and the cell lysates were harvested to detect luciferase activity. (A) Medium alone; EV71 at an MOI of 5, 10, or 50; and CpG ODN (10 μg/ml) were used to stimulate mTRL9/293 cells. (B) Supernatants from EV71-infected RD cells (sEV71-RD) were collected to stimulate 293 or mTLR9/293 cells. DNase-treated sEV7I-RD was used to digest DNA. (C) mTLR9/293 cells were stimulated with EV71 at an MOI of 50, sEV71-RD, sEV7I-RD treated with UV (sEV71-RD-UV), or heat-inactivated sEV7I-RD (sEV71-RD-Heated). The data are expressed as means and SD of three independent experiments. *, $P < 0.05$; **, $P < 0.01$.

RESULTS

EV71 infection induces NF-κB activation through TLR9. To investigate whether EV71 infection activates TLR9 signaling, mTLR9/293 cells were cotransfected with pNF-κB luc and pRL-TK. After 24 h, the cells were infected with EV71 at various MOIs, and luciferase activity was determined after another 24 h. Low luciferase activity was detected at an MOI of 50, but activity was undetectable at MOIs of less than 50 (Fig. 1A). The data indicate that EV71 infection may not activate TLR9 directly. Because a high EV71 MOI may lead to cell apoptosis, the activation of TLR9 at an MOI of 50 may be due to endogenous DNA release. To test this hypothesis, supernatants from EV71-infected RD cells (sEV71-RD) were used to stimulate mTLR9/293 cells. Figure 1B demonstrates that sEV71-RD induces NF-κB signaling through TLR9. However, the ability of sEV71-RD to activate TLR9 was disrupted in the presence of DNase. To exclude the possibility that live virus in sEV71-RD induces cell apoptosis and activates TLR9, sEV71-RD was pretreated with UV light or heat inactivated. The data indicate that sEV71-RD pretreated with UV light or extreme heat is still capable of activating NF-κB signaling through TLR9 (Fig. 1C). These data suggest that EV71 infection induces cell death and may release endogenous DNA, which can then act as a DAMP to activate TLR9.

Cytokine release from EV71-infected Flt3L-DCs was reduced in TLR9KO mice. The pDC population is the major producer of type I IFN during the initial immune response to viral infection, and TLR7 and TLR9 are frequently activated. EV71 infection led to the activation of TLR9; thus, we evaluated the effect of EV71 infection on pDCs from WT and TLR9KO mice. The pDCs were derived from Flt3L-DCs. The Flt3L-DCs were infected with EV71 at MOIs of 5 and 10, and the total RNA was isolated to determine the level of VP1 transcripts, which represents viral replication. We found that viral replication was increased in Flt3L-DCs from TLR9KO mice infected with EV71 compared with Flt3L-DCs collected from WT mice (Fig. 2A); this result was also observed in the presence of DNase. These findings may be due to a reduction in antiviral cytokines released from TLR9KO mice. Therefore, we quantified the levels of the major anti-virus cytokine, IFN-α, after infection of WT or TLR9KO Flt3L-DCs. We found that EV71 infection of Flt3L-DCs induced IFN-α secretion, but IFN-α levels were reduced in Flt3L-DCs from TLR9KO mice (Fig. 2B). In addition, the secretion of proinflammatory cytokines following

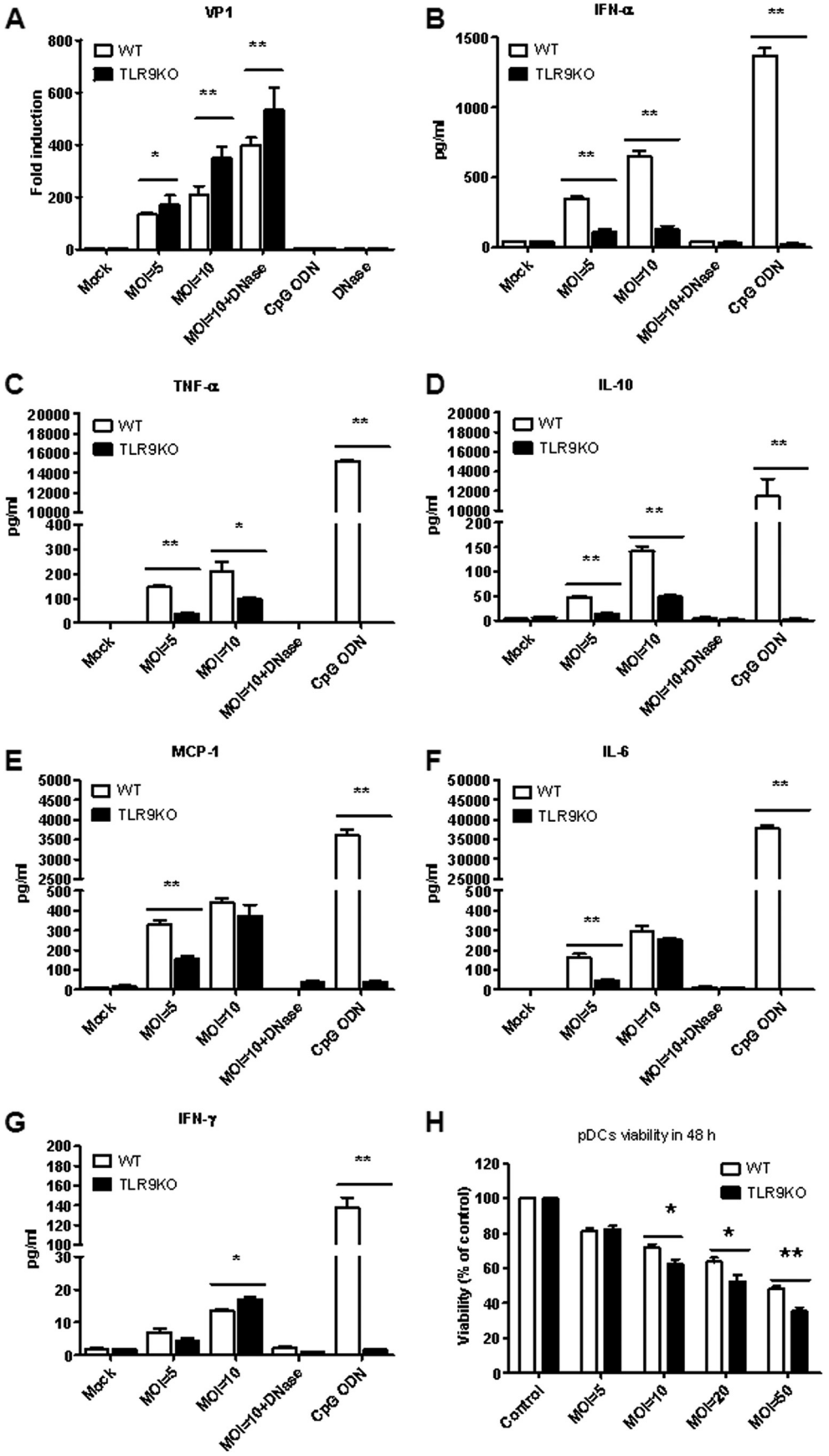
A
VP1
Fold induction
WT
TLR9KO
Mock
MOI=5
MOI=10
MOI=10+DNase
CpG ODN
DNase
B
IFN-α
pg/ml
C
TNF-α
D
IL-10
E
MCP-1
F
IL-6
G
IFN-γ
H
pDCs viability in 48 h
Viability (% of control)
Control
MOI=20
MOI=50

EV71 infection has been suggested to contribute to EV71 pathogenesis (3, 32, 37, 38).

We then quantified proinflammatory cytokine (TNF-α, IL-10, MCP-1, IL-6, IFN-γ, and IL-12) levels in Flt3L-DCs from WT and TLR9KO mice infected with EV71. TNF-α and IL-10 levels were reduced in Flt3L-DCs from TLR9KO mice at MOIs of 5 and 10 (Fig. 2C and D). MCP-1 and IL-6 levels were reduced in Flt3L-DCs from TLR9KO mice at an MOI of 5 but not at an MOI of 10 (Fig. 2E and F). In contrast, IFN-γ levels were increased in Flt3L-DCs from TLR9KO mice (Fig. 2G). IL-12 could not be detected after EV71 infection in Flt3L-DCs from WT or TLR9KO mice. The activation of these cytokines from Flt3L-DCs following treatment with sEV71-RD was lost in the presence of DNase. To confirm that EV71 infection of Flt3L-DCs induces cell death, cell viability was monitored at various MOIs. We observed that the viability of Flt3L-DCs was inversely proportional to the MOI. The viability of Flt3L-DCs from TLR9KO mice is lower than that of WT mice at high MOIs (Fig. 2H). These results suggest that EV71 infection induces endogenous DNA release, which can then activate pDCs through TLR9.

EV71 infection of 7-day-old TLR9KO mice induces neurological disease. EV71 infection induces DNA release, which activates Flt3L-DCs through TLR9; thus, TLR9 may play an important role in controlling EV71-mediated pathogenesis. To test this hypothesis, non-mouse-adapted EV71 strains 4643 and 5746 were used to infect WT or TLR9KO mice. Seven-day-old WT or TLR9KO mice were infected via i.p. injection with 10^7 PFU EV71. Loss of total body weight was observed in 7-day-old infected TLR9KO mice but not in WT mice (Fig. 3). Interestingly, the 7-day-old EV71-infected TLR9KO mice displayed clinical symptoms, including hunchback and limb weakness, which further progressed to hind-limb paralysis. Conversely, EV71-infected WT mice did not present with these clinical symptoms. Limb paralysis was initially slight at 3 days p.i., and severe paralysis of all limbs was observed at 7 days p.i. (Fig. 3). After 11 days p.i., the neurological manifestations of EV71-infected TLR9KO mice were no longer present, and 14-day-old infected TLR9KO mice did not exhibit any clinical symptoms (data not shown). Our observations suggest that TLR9 may play a role in host defense mechanisms against EV71 strains 4643 and 5746.

Histopathological examination of EV71-infected mice. Histopathological examinations of WT and TLR9KO mice at 3, 7, and 11 days p.i. were performed. Brain tissue presented focal minimal to slight perivascular cuffing, neural degeneration, demyelination, and gliosis in 7-day-old TLR9KO mice at 3, 7, and 11 days p.i.; brain tissues from WT mice displayed none of these histopathological features (Fig. 4). In the small intestine, moderate to severe villous atrophy with edema fluid accumulation in the lumen was observed in 7-day-old TLR9KO mice at 3 days p.i., and this clinical symptom improved slightly by 7 days p.i. Small intestine tissue from WT mice appeared normal. We also observed moderate to severe necrotizing myositis with fragmentation of myofibers and inflammatory cell infiltration in the forelimbs and hind limbs of 7-day-old TLR9KO mice at 7 days p.i., but equivalent tissues in WT mice were unaffected (Fig. 4).

EV71 replication was increased in EV71-infected TLR9KO mice. To further confirm that EV71 replication was increased in various organs following EV71 infection with 10^7 PFU, mice were euthanized at 3, 7, and 11 days p.i. to quantify viral titers. Viral titers from brain, intestine, lung, forelimb, and hind-limb tissues were measured by plaque assay. Viral titers in the brain, intestine, and lung tissues of TLR9KO mice were higher than titers in the equivalent tissues of WT mice at 7 days p.i. (Fig. 5A, B, and C). Moreover, viral titers in the forelimb and hind limb were higher than titers from the equivalent WT tissues at 3 and 7 days p.i. (Fig. 5D and E). Together, these data suggest that the virus travels from the gut to the intestines, but the number of infectious viral particles that reach the limb muscles is likely to be insufficient for detection by the plaque assay.

Proinflammatory cytokines are upregulated in brain tissues of infected TLR9KO mice. Several studies have addressed the elevated levels of cytokines and chemokines in children with brainstem encephalitis and pulmonary edema (3, 6, 37). To determine whether neurological manifestations are associated with increased cytokine and chemokine levels in brain tissue, the cytokine and chemokine levels were quantified from RNA transcripts collected from infected mice at 3, 7, and 11 days p.i. Consistently, the RNA transcript levels of several cytokines (TNF-α, IFN-γ, IL-6, and IL-1β) and chemokines (MIP-1α, MCP-1, and IP-10) were significantly elevated in EV71-infected 7-day-old TLR9KO mice compared with EV71-infected 7-day-old WT mice at 7 days p.i. (Fig. 6). The antiviral cytokine IFN-α5 was significantly increased in EV71-infected WT mice at 3 days p.i. compared with EV71-infected TLR9KO mice (Fig. 6C). These results may be explained by dysfunctional TLR9 signaling. However, the levels of IFN-α5 in TLR9KO mice at 7 and 11 days p.i. were 2- and 3-fold higher than IFN-α5 levels in WT mice at 7 and 11 days p.i., respectively (Fig. 6C). Additionally, the levels of the antiviral cytokines IFN-γ and IL-1β were 2- to 3-fold higher in TLR9KO mice at 7 and 11 days p.i. than in WT mice at the same time points (Fig. 6B and E). In contrast, levels of inflammatory cytokines (TNF-α and IL-6) and chemokines (MIP-1α and MCP-1) were 5- to 10-fold higher in EV71-infected TLR9KO mice than in WT mice (Fig. 6A, D, F, and G). Interestingly, IP-10 levels in EV71-infected TLR9KO mice increased by 500-fold at 3 and 7 days p.i. compared with WT mice (Fig. 6H). These data indicate that IL-10 may play an important role in EV71-mediated pathogenesis.

Roles of plasmacytoid dendritic cells in EV71 infection. Because TLR9 is highly expressed in pDCs, the expression levels of TLR9 in neonatal or adult mice may have effects on the protective immune responses. To determine the expression levels of TLRs in pDCs, pDCs ($PDCA1^+$ cells) were isolated from neonatal or adult mice to detect the expression of TLRs. We found that TLR1, -2, -7, and -9 expression was detected in pDCs. Although the expression

FIG 2 EV71 infection of Flt3L-DCs from TLR9KO mice leads to increased viral replication and cytokine production. (A) Flt3L-DCs from WT and TLR9KO mice were cultured with EV71 at an MOI of 5 or 10 for 48 h. CpG ODN (10 μg/ml) was used as a positive control. The mRNA levels of EV71 VP1 were used as an indicator of viral replication. (B) The level of IFN-α was detected by cytokine ELISA (eBioscience, CA, USA). (C to G) TNF-α (C), IL-10 (D), MCP-1 (E), IL-6 (F), and IFN-γ (G) in culture supernatants were measured by Cytometric Bead Array (BD Bioscience, CA, USA) using a flow cytometer. (H) EV71 infection induced the death of pDCs in WT and TLR9KO mice. The pDCs were seeded at 5×10^5/well in 48 wells in a total volume of 500 μl and infected with EV71 at MOIs of 5, 10, 20, and 50. Cell viability was determined by trypan blue exclusion assay at 48 h. The data are expressed as means and SD of three independent experiments. *, $P < 0.05$; **, $P < 0.01$.

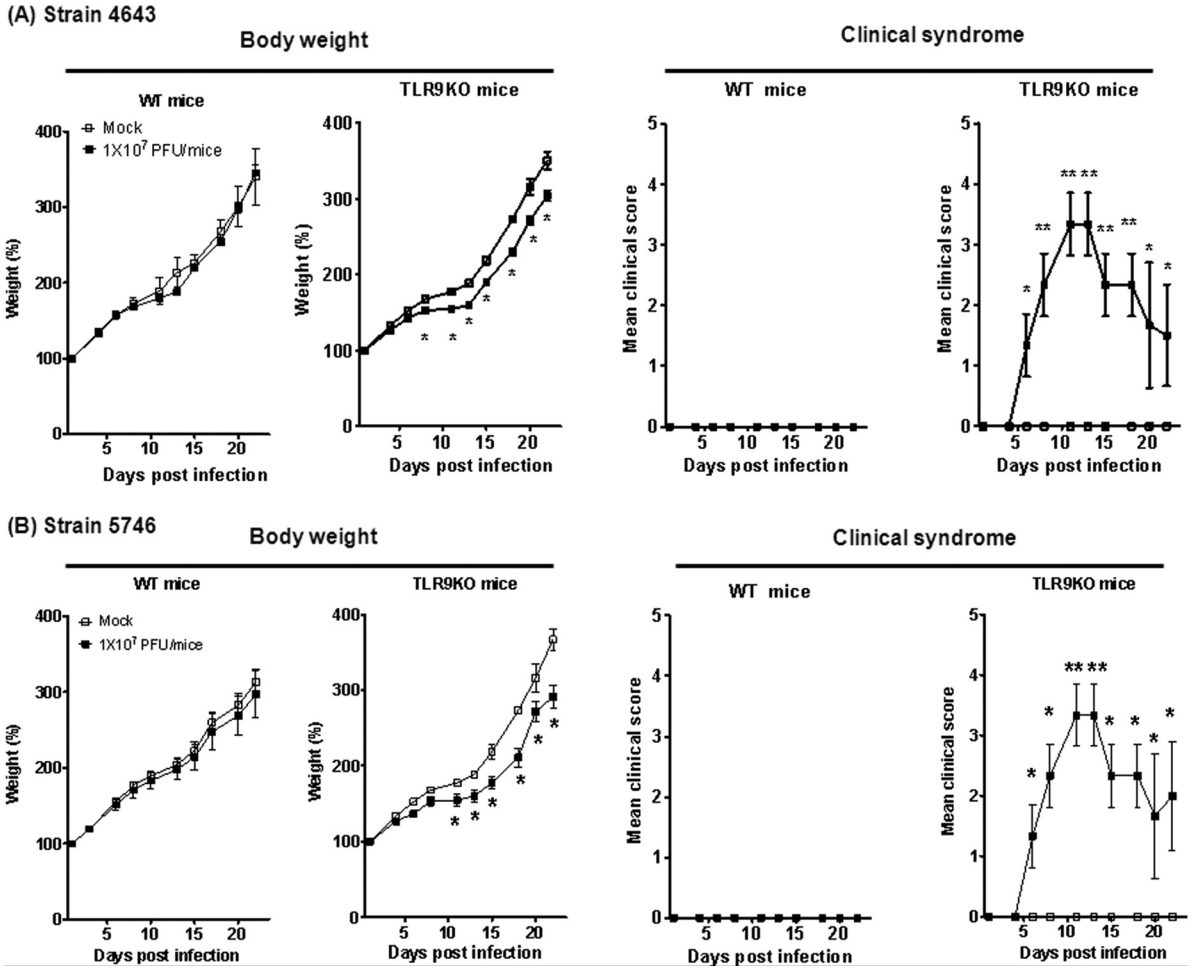

FIG 3 Seven-day-old WT or TLR9KO mice were infected via i.p. injection with 10^7 PFU EV71 strain 4643 (A) or 5746 (B). Body weight changes and clinical symptoms of the infected mice were monitored every 2 to 3 days. The clinical scores were defined as follows: 0, healthy; 1, ruffled hair and hunchbacked; 2, limb weakness; 3, paralysis in 1 limb; 4, paralysis in both limbs; and 5, death. Control mice were injected with PBS. Each group consisted of 6 or 7 mice. The error bars indicate SD.

of TLR9 in adult mice appeared higher than that in neonatal mice, it was not statistically significant (Fig. 7A). Thus, the induction of neurological manifestations is not due to different expression levels of TLR9 in neonatal and adult mice. To further investigate whether pDCs are potentially involved in the protective mechanisms, 7-day-old mice were treated with anti-PDCA1 antibody to deplete pDCs before EV71 infection. We observed that the PDCA1-depleted mice had a more severe neurological syndrome than control antibody-treated mice after EV71 infection (Fig. 7B). pDCs may play critical roles in protective mechanisms during EV71 infection.

DISCUSSION

TLR3 and RIG-I are major innate immune receptors that recognize viral components during EV71 infection, although other innate immune receptors may also protect the host against EV71 infection. In this report, we demonstrated that endogenous DNA released from EV71-infected cells can activate TLR9, and this mechanism may be protective against EV71 infection. We found that 7-day-old TLR9KO mice infected with non-mouse-adapted EV71 presented with neurological disease manifestations, but WT mice did not exhibit these symptoms (Fig. 3). However, no clinical symptoms were observed when 14-day-old TLR9KO mice were infected with EV71. In contrast, EV71-infected 14-day-old AG129 mice displayed progressive limb paralysis prior to death (19). These findings suggest that interferon is critical for controlling EV71 infection. In addition to the direct recognition of EV71 infection by TLR3 and RIG-I, which mediates the release of interferon, we demonstrated that IFN-α could be produced following indirect recognition of EV71 infection by TLR9.

It is now evident that DAMPs are released during cellular injury and activate proinflammatory pathways (29). These DAMPs activate immune responses through different innate receptors, which can then subsequently activate the adaptive immune response. Endogenous nucleosomes and DNA are released from necrotic cells and have been shown to stimulate DCs directly to promote their maturation and induce cytokine secretion (39, 40). Moreover, endogenous DNA and chromatin complexes are capable of activating DCs via TLR9-dependent or -independent mechanisms (41, 42). EV71 infection induces apoptosis in epithelial cells (43), endothelial cells (28), and neuronal cells (28). Accordingly, we demonstrated that sEV71-RD activates TLR9 signaling,

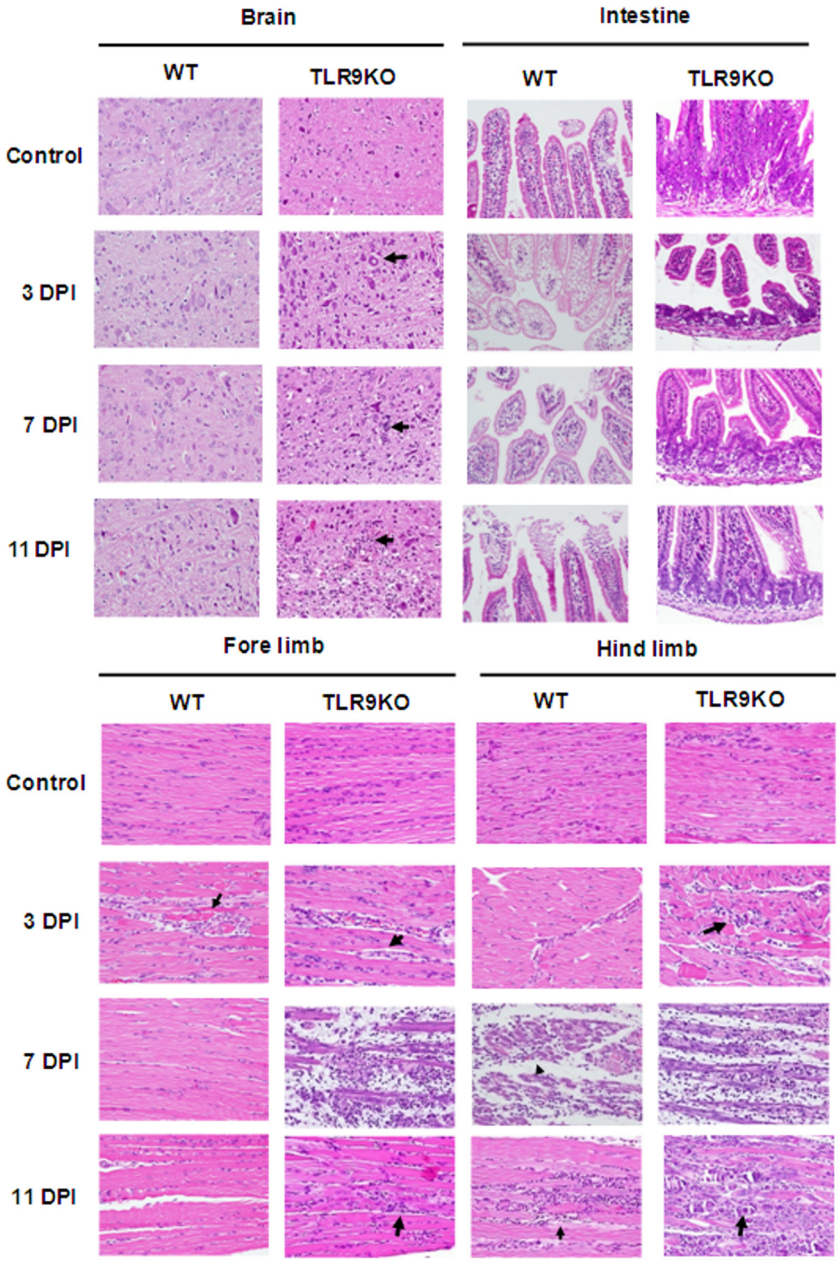

FIG 4 Histological examination of various organs from EV-71-infected mice. Seven-day-old WT and TLR9KO mice were infected via i.p. injection of EV71 at 10^7 PFU. The animals were euthanized at 3, 7, and 11 days postinfection (DPI), and paraffin-embedded tissue sections of the organs were stained with H&E. The specimens are representative of 3 mice in each group, with similar histologies. Tissue damage was identified by a pathologist and is indicated by arrows (magnification, ×400).

but this signal activation was lost when cells were pretreated with DNase (Fig. 1). EV71 infection of pDCs from WT mice induces IFN-α production, but infected pDCs from TLR9KO mice did not produce IFN-α (Fig. 2). These data clearly indicate that EV71-mediated cell death activates TLR9 signaling to secrete IFN-α and prevent viral replication. Moreover, neurological manifestations were observed in EV71-infected 7-day-old TLR9KO mice, but not in 14-day-old mice (Fig. 3). The isolated pDCs ($PDCA1^+$ cells) from neonatal or adult mice were used to detect the expression of TLRs. We found that the TLR expression levels were comparable in neonatal and adult mice (Fig. 7A). Thus, the induction of neurological manifestations may not be due to different expression levels of TLR9 in neonatal and adult mice. However, neonatal pDCs are impaired in their ability to mature and produce the levels of IFN-α common in adult mice (44, 45). Furthermore, we confirmed that pDCs are involved in protective mechanisms by using anti-PDCA1 antibody to deplete pDCs before EV71 infection. However, we cannot exclude the possibility that other TLR9-expressing cells (i.e., B cells or monocytes) also play some roles during EV71 infection.

The production of proinflammatory cytokines is initiated following stimulation in an autocrine manner, which acts to regulate

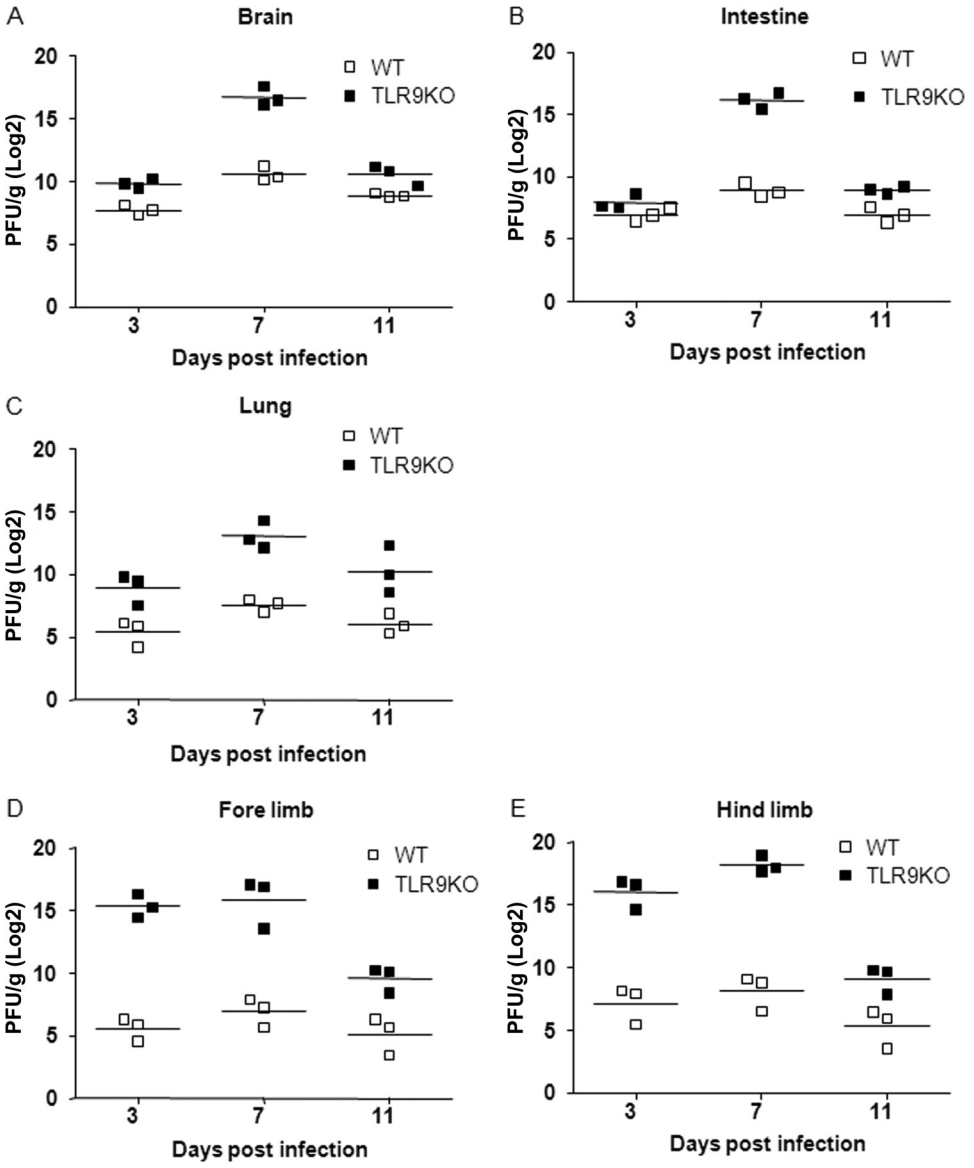

FIG 5 Viral titers were determined in the organs of EV71-infected WT and TLR9KO mice. Seven-day-old WT and TLR9KO mice were infected via i.p. injection of EV71 at 10^7 PFU. At 3, 7, and 11 days postinfection; the mice were euthanized, and viral titers in the brain (A), intestine (B), lung (C), forelimb (D), and hind limb (E) were determined by plaque assay. The results are expressed as PFU per gram of tissue. The horizontal line indicates the mean of each group.

the immune inflammatory response (46). Therefore, the balance between pro- and anti-inflammatory cytokines is critical, and determining the ratios of major pro- and anti-inflammatory cytokines helps determine the inflammatory status of an infected individual. Elevated levels of several cytokines and chemokines have been reported in children with brainstem encephalitis and pulmonary edema (3, 6, 37). Similarly, the levels of the proinflammatory cytokines implicated in EV71 infection, including IL-1α, IL-10, MIP-2, TNF-α, and IFN-α, were significantly elevated in 7-day-old TLR9KO mice compared with WT mice.

IFN-α plays an important role in the host defense against EV71 infection and is responsible for the earlier detection of viral involvement in the central nervous system (47). Interestingly, high levels of IP-10 were observed in brain tissue from TLR9KO mice, but not in the equivalent WT tissue. IP-10 was identified as a proinflammatory chemokine that mediates leukocyte trafficking and subsequently activates T lymphocytes, NK cells, macrophages, dendritic cells, and B cells (48). The increased expression of IP-10 occurs prior to the development of clinical symptoms in brain tissues of neonatal mice infected with virulent (Fr98) polytropic murine retrovirus (49). The IP-10 levels were positively correlated with organ damage and pathogen burden in hepatitis C virus (HCV)-HIV-coinfected patients (50). IP-10 levels were much higher in cerebrospinal fluid than in plasma from EV71-infected patients with neurological damage (51). High levels of IP-10 were induced by EV71 infection in a mouse model, and infection led to the recruitment of $CD8^+$ T cells and increased IFN-γ levels to eliminate the virus from infected tissues (52). Induction of IP-10 in TLRKO mice after EV71 infection may be one mechanism that protects infected mice from severe brain damage.

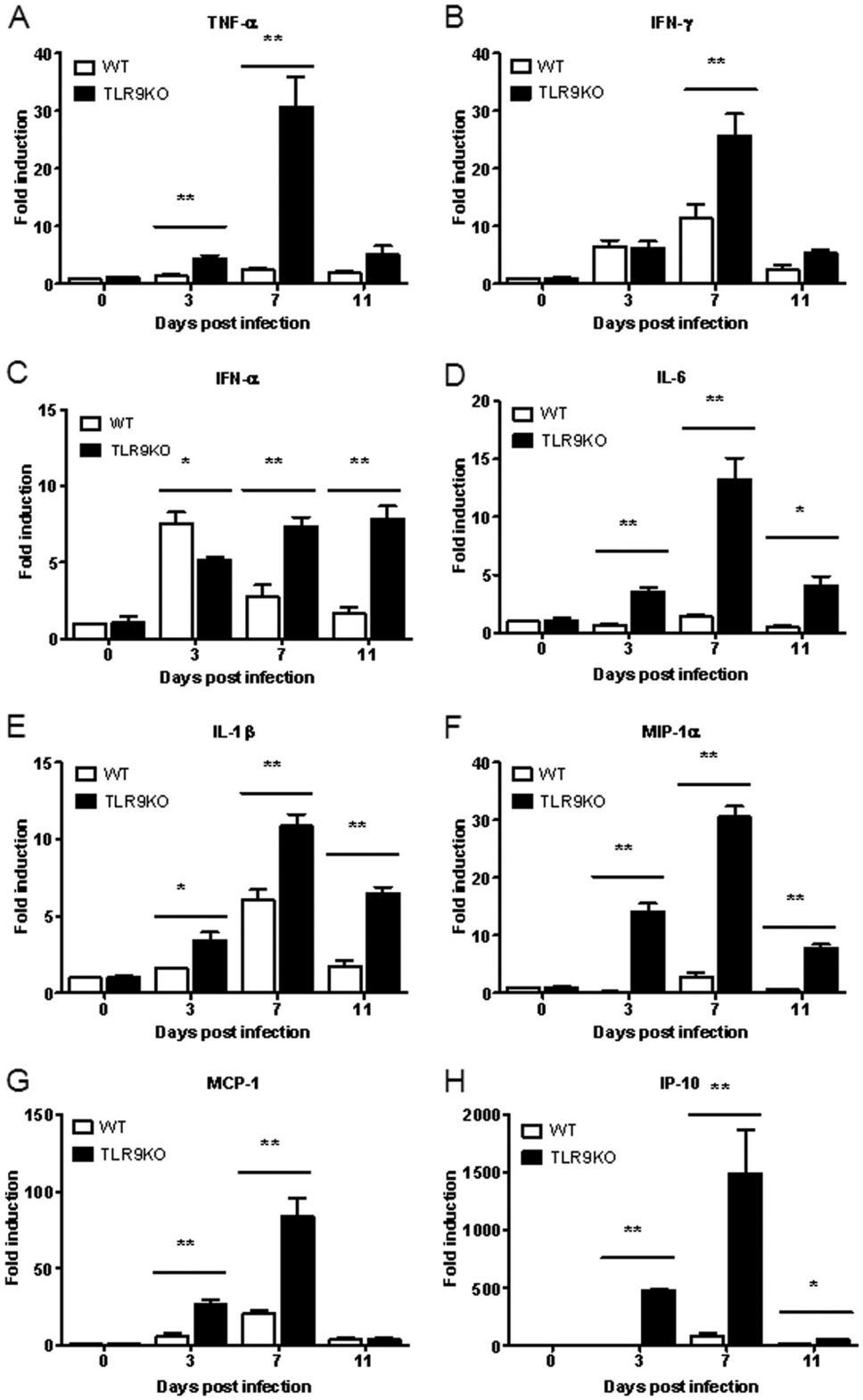

FIG 6 Cytokine and chemokine expression in EV71-infected brains of WT and TLR9KO mice. Seven-day-old WT and TLR9KO mice were infected via i.p. injection with EV71 at 10^7 PFU. At 3, 7, and 11 days postinfection, the mice were euthanized, and brain tissues were collected. The expression levels of TNF-α (A), IFN-γ (B), IFN-α (C), IL-6 (D), IL-1β (E), MIP-1α (F), MCP-1 (G), and IP-10 (H) in the brain were quantified by real-time qPCR. The data are expressed as means and SD of three independent experiments. *, $P < 0.05$; **, $P < 0.01$.

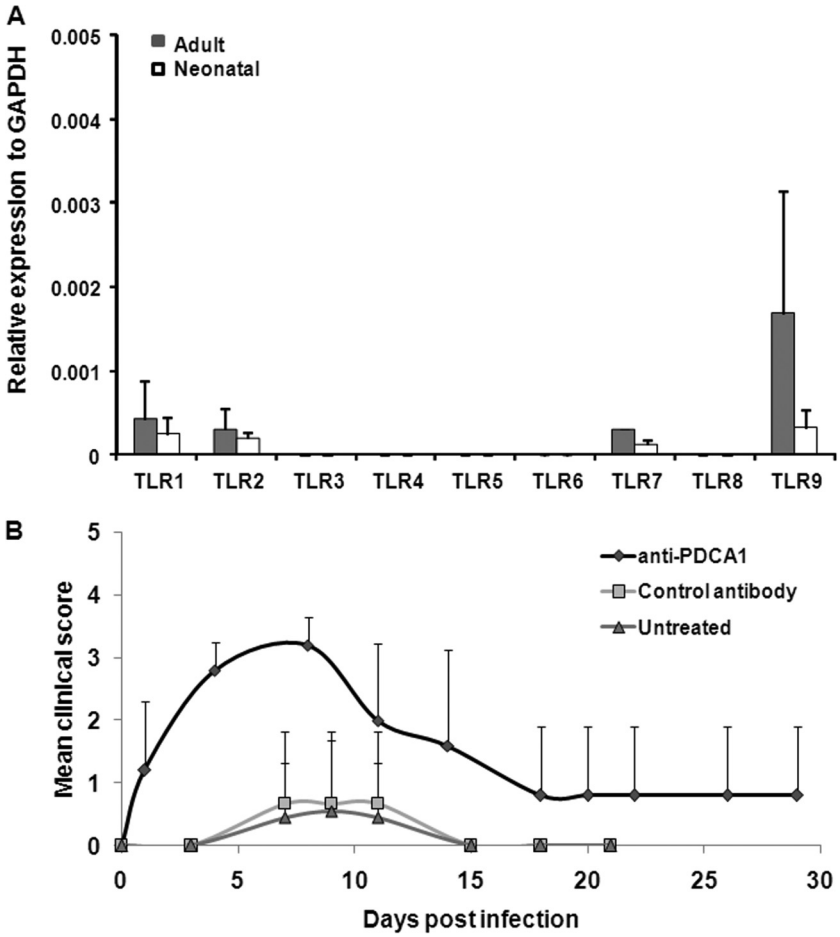

FIG 7 Roles of pDCs in EV71 infection. (A) TLR gene expression in adult and neonatal pDCs. The cDNAs of adult (6-week-old) and neonatal (7-day-old) pDCs were isolated from wild-type mice using an anti-mPDCA1 microbead kit according to the procedures provided by the manufacturer (Miltenyi Biotec). Total RNA was extracted from pDCs using TRIzol reagent, and 1 μg of RNA was reversed transcribed to cDNA for detecting the transcripts of TLRs. Expression levels of TLR1 to -9 were assessed using a real-time qPCR assay. The data represent the mean real-time qPCR expression and SD from 3 different animals. (B) Seven-day-old pDC-depleted mice were infected with EV71 strain 4643. Antibody-treated 5-day-old mice (treated with anti-mouse CD317 antibody or control antibody) or untreated mice were infected with 1×10^7 PFU of EV71 at day 7. Clinical symptoms were monitored every 2 to 4 days. Each group included 3 to 9 mice, and all of the experiments were repeated with similar results.

Unlike EV71 infection in AG129 mice, infection of EV71 in 7-day-old TLR9KO mice is not fatal.

In conclusion, we demonstrated that 7-day-old TLR9KO mice are susceptible to non-mouse-adapted EV71 infection, and these mice exhibit clinical neurological symptoms similar to those observed in patients. Most importantly, we found that the TLR9 signaling pathway could provide protection against EV71 infection via the production of DAMPs.

ACKNOWLEDGMENTS

We thank Jiunn-Wang Liao from the Graduate Institute of Veterinary Pathobiology, National Chung Hsing University, Taichung, Taiwan, Republic of China, and the Pathology Core Laboratory of the National Health Research Institutes for pathological analysis.

This work was supported by a grant from the National Science Council awarded to S.-I.L. (NSC 100-2325-B-400-015).

We declare no financial or commercial conflicts of interest.

REFERENCES

1. **AbuBakar S, Chee HY, Al-Kobaisi MF, Xiaoshan J, Chua KB, Lam SK.** 1999. Identification of enterovirus 71 isolates from an outbreak of hand, foot and mouth disease (HFMD) with fatal cases of encephalomyelitis in Malaysia. Virus Res. **61:**1–9.
2. **Ho M, Chen ER, Hsu KH, Twu SJ, Chen KT, Tsai SF, Wang JR, Shih SR.** 1999. An epidemic of enterovirus 71 infection in Taiwan. Taiwan Enterovirus Epidemic Working Group. N. Engl. J. Med. **341:**929–935.
3. **Lin TY, Hsia SH, Huang YC, Wu CT, Chang LY.** 2003. Proinflammatory cytokine reactions in enterovirus 71 infections of the central nervous system. Clin. Infect. Dis. **36:**269–274. http://dx.doi.org/10.1086/345905.
4. **Wong SS, Yip CC, Lau SK, Yuen KY.** 2010. Human enterovirus 71 and hand, foot and mouth disease. Epidemiol. Infect. **138:**1071–1089. http://dx.doi.org/10.1017/S0950268809991555.
5. **Liu CC, Tseng HW, Wang SM, Wang JR, Su IJ.** 2000. An outbreak of enterovirus 71 infection in Taiwan, 1998: epidemiologic and clinical manifestations. J. Clin. Virol. **17:**23–30. http://dx.doi.org/10.1016/S1386-6532(00)00068-8.
6. **Wang SM, Lei HY, Huang KJ, Wu JM, Wang JR, Yu CK, Su IJ, Liu CC.** 2003. Pathogenesis of enterovirus 71 brainstem encephalitis in pediatric patients: roles of cytokines and cellular immune activation in patients with pulmonary edema. J. Infect. Dis. **188:**564–570. http://dx.doi.org/10.1086/376998.
7. **Solomon T, Lewthwaite P, Perera D, Cardosa MJ, McMinn P, Ooi MH.** 2010. Virology, epidemiology, pathogenesis, and control of enterovirus 71. Lancet Infect. Dis. **10:**778–790. http://dx.doi.org/10.1016/S1473-3099(10)70194-8.

8. **Chen TC, Lai YK, Yu CK, Juang JL.** 2007. Enterovirus 71 triggering of neuronal apoptosis through activation of Abl-Cdk5 signalling. Cell Microbiol. **9:**2676–2688. http://dx.doi.org/10.1111/j.1462-5822.2007.00988.x.
9. **Chi C, Sun Q, Wang S, Zhang Z, Li X, Cardona CJ, Jin Y, Xing Z.** 2013. Robust antiviral responses to enterovirus 71 infection in human intestinal epithelial cells. Virus Res. **176:**53–60. http://dx.doi.org/10.1016/j.virusres.2013.05.002.
10. **Weng KF, Chen LL, Huang PN, Shih SR.** 2010. Neural pathogenesis of enterovirus 71 infection. Microbes Infect. **12:**505–510. http://dx.doi.org/10.1016/j.micinf.2010.03.006.
11. **O'Neill LA, Bowie AG.** 2010. Sensing and signaling in antiviral innate immunity. Curr. Biol. **20:**R328–R333. http://dx.doi.org/10.1016/j.cub.2010.01.044.
12. **Kato H, Takeuchi O, Sato S, Yoneyama M, Yamamoto M, Matsui K, Uematsu S, Jung A, Kawai T, Ishii KJ, Yamaguchi O, Otsu K, Tsujimura T, Koh CS, Reis e Sousa C, Matsuura Y, Fujita T, Akira S.** 2006. Differential roles of MDA5 and RIG-I helicases in the recognition of RNA viruses. Nature **441:**101–105. http://dx.doi.org/10.1038/nature04734.
13. **Takahasi K, Yoneyama M, Nishihori T, Hirai R, Kumeta H, Narita R, Gale M, Jr, Inagaki F, Fujita T.** 2008. Nonself RNA-sensing mechanism of RIG-I helicase and activation of antiviral immune responses. Mol. Cell **29:**428–440. http://dx.doi.org/10.1016/j.molcel.2007.11.028.
14. **Oshiumi H, Matsumoto M, Funami K, Akazawa T, Seya T.** 2003. TICAM-1, an adaptor molecule that participates in Toll-like receptor 3-mediated interferon-beta induction. Nat. Immunol. **4:**161–167. http://dx.doi.org/10.1038/ni886.
15. **Uematsu S, Sato S, Yamamoto M, Hirotani T, Kato H, Takeshita F, Matsuda M, Coban C, Ishii KJ, Kawai T, Takeuchi O, Akira S.** 2005. Interleukin-1 receptor-associated kinase-1 plays an essential role for Toll-like receptor (TLR)7- and TLR9-mediated interferon-{alpha} induction. J. Exp. Med. **201:**915–923. http://dx.doi.org/10.1084/jem.20042372.
16. **Barber GN.** 2011. Cytoplasmic DNA innate immune pathways. Immunol. Rev. **243:**99–108. http://dx.doi.org/10.1111/j.1600-065X.2011.01051.x.
17. **Nace G, Evankovich J, Eid R, Tsung A.** 2012. Dendritic cells and damage-associated molecular patterns: endogenous danger signals linking innate and adaptive immunity. J. Innate Immun. **4:**6–15. http://dx.doi.org/10.1159/000334245.
18. **Bianchi ME.** 2007. DAMPs, PAMPs and alarmins: all we need to know about danger. J. Leukoc. Biol. **81:**1–5. http://dx.doi.org/10.1189/jlb.0306164.
19. **Khong WX, Yan B, Yeo H, Tan EL, Lee JJ, Ng JK, Chow VT, Alonso S.** 2012. A non-mouse-adapted enterovirus 71 (EV71) strain exhibits neurotropism, causing neurological manifestations in a novel mouse model of EV71 infection. J. Virol. **86:**2121–2131. http://dx.doi.org/10.1128/JVI.06103-11.
20. **Lei X, Liu X, Ma Y, Sun Z, Yang Y, Jin Q, He B, Wang J.** 2010. The 3C protein of enterovirus 71 inhibits retinoid acid-inducible gene I-mediated interferon regulatory factor 3 activation and type I interferon responses. J. Virol. **84:**8051–8061. http://dx.doi.org/10.1128/JVI.02491-09.
21. **Wang B, Xi X, Lei X, Zhang X, Cui S, Wang J, Jin Q, Zhao Z.** 2013. Enterovirus 71 protease 2Apro targets MAVS to inhibit anti-viral type I interferon responses. PLoS Pathog. **9:**e1003231. http://dx.doi.org/10.1371/journal.ppat.1003231.
22. **Hornung V, Schlender J, Guenthner-Biller M, Rothenfusser S, Endres S, Conzelmann KK, Hartmann G.** 2004. Replication-dependent potent IFN-alpha induction in human plasmacytoid dendritic cells by a single-stranded RNA virus. J. Immunol. **173:**5935–5943. http://dx.doi.org/10.4049/jimmunol.173.10.5935.
23. **Wang Y, Swiecki M, McCartney SA, Colonna M.** 2011. dsRNA sensors and plasmacytoid dendritic cells in host defense and autoimmunity. Immunol. Rev. **243:**74–90. http://dx.doi.org/10.1111/j.1600-065X.2011.01049.x.
24. **Kadowaki N, Ho S, Antonenko S, Malefyt RW, Kastelein RA, Bazan F, Liu YJ.** 2001. Subsets of human dendritic cell precursors express different Toll-like receptors and respond to different microbial antigens. J. Exp. Med. **194:**863–869. http://dx.doi.org/10.1084/jem.194.6.863.
25. **Koyama S, Ishii KJ, Coban C, Akira S.** 2008. Innate immune response to viral infection. Cytokine **43:**336–341. http://dx.doi.org/10.1016/j.cyto.2008.07.009.
26. **Kaisho T.** 2012. Pathogen sensors and chemokine receptors in dendritic cell subsets. Vaccine **30:**7652–7657. http://dx.doi.org/10.1016/j.vaccine.2012.10.043.
27. **Li ML, Hsu TA, Chen TC, Chang SC, Lee JC, Chen CC, Stollar V, Shih SR.** 2002. The 3C protease activity of enterovirus 71 induces human neural cell apoptosis. Virology **293:**386–395. http://dx.doi.org/10.1006/viro.2001.1310.
28. **Liang CC, Sun MJ, Lei HY, Chen SH, Yu CK, Liu CC, Wang JR, Yeh TM.** 2004. Human endothelial cell activation and apoptosis induced by enterovirus 71 infection. J. Med. Virol. **74:**597–603. http://dx.doi.org/10.1002/jmv.20216.
29. **Chen GY, Nunez G.** 2010. Sterile inflammation: sensing and reacting to damage. Nat. Rev. Immunol. **10:**826–837. http://dx.doi.org/10.1038/nri2873.
30. **Yan JJ, Su IJ, Chen PF, Liu CC, Yu CK, Wang JR.** 2001. Complete genome analysis of enterovirus 71 isolated from an outbreak in Taiwan and rapid identification of enterovirus 71 and coxsackievirus A16 by RT-PCR. J. Med. Virol. **65:**331–339. http://dx.doi.org/10.1002/jmv.2038.
31. **Liu CC, Lian WC, Butler M, Wu SC.** 2007. High immunogenic enterovirus 71 strain and its production using serum-free microcarrier Vero cell culture. Vaccine **25:**19–24. http://dx.doi.org/10.1016/j.vaccine.2006.06.083.
32. **Gong X, Zhou J, Zhu W, Liu N, Li J, Li L, Jin Y, Duan Z.** 2012. Excessive proinflammatory cytokine and chemokine responses of human monocyte-derived macrophages to enterovirus 71 infection. BMC Infect. Dis. **12:**224. http://dx.doi.org/10.1186/1471-2334-12-224.
33. **Wu CN, Lin YC, Fann C, Liao NS, Shih SR, Ho MS.** 2001. Protection against lethal enterovirus 71 infection in newborn mice by passive immunization with subunit VP1 vaccines and inactivated virus. Vaccine **20:**895–904. http://dx.doi.org/10.1016/S0264-410X(01)00385-1.
34. **Tong X, Zhang L, Hu M, Leng J, Yu B, Zhou B, Hu Y, Zhang Q.** 2009. The mechanism of chemokine receptor 9 internalization triggered by interleukin 2 and interleukin 4. Cell Mol. Immunol. **6:**181–189. http://dx.doi.org/10.1038/cmi.2009.25.
35. **Tian J, Avalos AM, Mao SY, Chen B, Senthil K, Wu H, Parroche P, Drabic S, Golenbock D, Sirois C, Hua J, An LL, Audoly L, La Rosa G, Bierhaus A, Naworth P, Marshak-Rothstein A, Crow MK, Fitzgerald KA, Latz E, Kiener PA, Coyle AJ.** 2007. Toll-like receptor 9-dependent activation by DNA-containing immune complexes is mediated by HMGB1 and RAGE. Nat. Immunol. **8:**487–496. http://dx.doi.org/10.1038/ni1457.
36. **Davidson S, Kaiko G, Loh Z, Lalwani A, Zhang V, Spann K, Foo SY, Hansbro N, Uematsu S, Akira S, Matthaei KI, Rosenberg HF, Foster PS, Phipps S.** 2011. Plasmacytoid dendritic cells promote host defense against acute pneumovirus infection via the TLR7-MyD88-dependent signaling pathway. J. Immunol. **186:**5938–5948. http://dx.doi.org/10.4049/jimmunol.1002635.
37. **Wang SM, Lei HY, Yu CK, Wang JR, Su IJ, Liu CC.** 2008. Acute chemokine response in the blood and cerebrospinal fluid of children with enterovirus 71-associated brainstem encephalitis. J. Infect. Dis. **198:**1002–1006. http://dx.doi.org/10.1086/591462.
38. **Khong WX, Foo DG, Trasti SL, Tan EL, Alonso S.** 2011. Sustained high levels of interleukin-6 contribute to the pathogenesis of enterovirus 71 in a neonate mouse model. J. Virol. **85:**3067–3076. http://dx.doi.org/10.1128/JVI.01779-10.
39. **Lande R, Gregorio J, Facchinetti V, Chatterjee B, Wang YH, Homey B, Cao W, Su B, Nestle FO, Zal T, Mellman I, Schroder JM, Liu YJ, Gilliet M.** 2007. Plasmacytoid dendritic cells sense self-DNA coupled with antimicrobial peptide. Nature **449:**564–569. http://dx.doi.org/10.1038/nature06116.
40. **Decker P, Singh-Jasuja H, Haager S, Kotter I, Rammensee HG.** 2005. Nucleosome, the main autoantigen in systemic lupus erythematosus, induces direct dendritic cell activation via a MyD88-independent pathway: consequences on inflammation. J. Immunol. **174:**3326–3334. http://dx.doi.org/10.4049/jimmunol.174.6.3326.
41. **Yasuda K, Yu P, Kirschning CJ, Schlatter B, Schmitz F, Heit A, Bauer S, Hochrein H, Wagner H.** 2005. Endosomal translocation of vertebrate DNA activates dendritic cells via TLR9-dependent and -independent pathways. J. Immunol. **174:**6129–6136. http://dx.doi.org/10.4049/jimmunol.174.10.6129.
42. **Boule MW, Broughton C, Mackay F, Akira S, Marshak-Rothstein A, Rifkin IR.** 2004. Toll-like receptor 9-dependent and -independent dendritic cell activation by chromatin-immunoglobulin G complexes. J. Exp. Med. **199:**1631–1640. http://dx.doi.org/10.1084/jem.20031942.
43. **Kuo RL, Kung SH, Hsu YY, Liu WT.** 2002. Infection with enterovirus 71

or expression of its 2A protease induces apoptotic cell death. J. Gen. Virol. **83:**1367–1376.

44. **Zhang X, Lepelley A, Azria E, Lebon P, Roguet G, Schwartz O, Launay O, Leclerc C, Lo-Man R.** 2013. Neonatal plasmacytoid dendritic cells (pDCs) display subset variation but can elicit potent anti-viral innate responses. PLoS One **8:**e52003. http://dx.doi.org/10.1371/journal.pone.0052003.
45. **Gold MC, Donnelly E, Cook MS, Leclair CM, Lewinsohn DA.** 2006. Purified neonatal plasmacytoid dendritic cells overcome intrinsic maturation defect with TLR agonist stimulation. Pediatr. Res. **60:**34–37. http://dx.doi.org/10.1203/01.pdr.0000220352.13547.f4.
46. **Girndt M, Kohler H.** 2003. Interleukin-10 (IL-10): an update on its relevance for cardiovascular risk. Nephrol. Dial. Transplant. **18:**1976–1979. http://dx.doi.org/10.1093/ndt/gfg311.
47. **Liu ML, Lee YP, Wang YF, Lei HY, Liu CC, Wang SM, Su IJ, Wang JR, Yeh TM, Chen SH, Yu CK.** 2005. Type I interferons protect mice against enterovirus 71 infection. J. Gen. Virol. **86:**3263–3269. http://dx.doi.org/10.1099/vir.0.81195-0.
48. **Liu M, Guo S, Hibbert JM, Jain V, Singh N, Wilson NO, Stiles JK.** 2011. CXCL10/IP-10 in infectious diseases pathogenesis and potential therapeutic implications. Cytokine Growth Factor Rev. **22:**121–130. http://dx.doi.org/10.1016/j.cytogfr.2011.06.001.
49. **Peterson KE, Robertson SJ, Portis JL, Chesebro B.** 2001. Differences in cytokine and chemokine responses during neurological disease induced by polytropic murine retroviruses map to separate regions of the viral envelope gene. J. Virol. **75:**2848–2856. http://dx.doi.org/10.1128/JVI.75.6.2848-2856.2001.
50. **Roe B, Coughlan S, Hassan J, Grogan A, Farrell G, Norris S, Bergin C, Hall WW.** 2007. Elevated serum levels of interferon-gamma-inducible protein-10 in patients coinfected with hepatitis C virus and HIV. J. Infect. Dis. **196:**1053–1057. http://dx.doi.org/10.1086/520935.
51. **Zhang Y, Liu H, Wang L, Yang F, Hu Y, Ren X, Li G, Yang Y, Sun S, Li Y, Chen X, Li X, Jin Q.** 2013. Comparative study of the cytokine/chemokine response in children with differing disease severity in enterovirus 71-induced hand, foot, and mouth disease. PLoS One **8:**e67430. http://dx.doi.org/10.1371/journal.pone.0067430.
52. **Shen FH, Tsai CC, Wang LC, Chang KC, Tung YY, Su IJ, Chen SH.** 2013. Enterovirus 71 infection increases expression of interferon-gamma-inducible protein 10 which protects mice by reducing viral burden in multiple tissues. J. Gen. Virol. **94:**1019–1027. http://dx.doi.org/10.1099/vir.0.046383-0.